Estimating the salinity of subglacial lakes from aerogeophysical data

Michael Studinger

Lamont-Doherty Earth Observatory of Columbia University, 61 Route 9W, Palisades, NY 10964, USA, mstuding@ldeo.columbia.edu

Summary The widespread occurrence of more than 145 lakes underneath the Antarctic ice sheet demonstrates that these aquatic ecosystems are an important part of the subglacial hydrosphere. The recent discovery of water flux between subglacial lakes beneath the East and West Antarctic ice sheet on timescales of several years indicates interconnectedness within the subglacial hydrological network and the potential for catastrophic drainage into the ocean. Subglacial lakes are now being recognized as an integral part of the global cryosphere and the global climate system. Knowledge of the physical, chemical and biological processes operating within these features is crucial for addressing questions about the presence and functioning of life in subglacial lakes. However, little is known about the prevailing *in situ* environmental conditions. Existing airborne ice-penetrating radar and laser altimeter data over large subglacial lakes can be used to estimate the salinity without penetrating the lakes.

Citation: Studinger, M., (2007), Estimating the salinity of subglacial lakes from aerogeophysical data, in Antarctica: A Keystone in a Changing World – Online Proceedings of the 10th ISAES X, edited by A. K. Cooper and C. R. Raymond et al., USGS Open-File Report 2007-1047, Extended Abstract 032, 4 p.

Introduction: The hydrological potential of subglacial lakes

Subglacial lakes are now being recognized as an integral part of the global cryosphere and the global climate system. The recent discovery of water flux between subglacial lakes beneath the East and West Antarctic ice sheets on timescales of several years indicates interconnectedness within the subglacial hydrological network.

The exact nature of the biological, physical and chemical conditions within subglacial Lake Vostok (105°E, 77°S) and other large lakes are still a matter of debate and await direct sampling of the lake water. Analysis of accreted ice samples, geophysical remote sensing and numerical modeling of water circulation can provide important background information on the chemical and biological conditions expected in Lake Vostok and other subglacial lakes.

The underlying assumption for estimating the salinity from aerogeophysical data is that the ice sheet above large subglacial lakes is in hydrostatic equilibrium and the hydrological potential of the lake surface is constant. Similar to the fluid potential of subaerial lakes, the hydrological potential Φ of a subglacial lake can be defined as:

$$\Phi = p_{ice} + \rho_{water}\, g\, Z_{lake} = \rho_{ice}\, g\, (Z_s - Z_{lake}) + \rho_{water}\, g\, Z_{lake} \qquad (1)$$

with p_{ice} being the ice overburden pressure, g = 9.81 m/s^2 the gravitational acceleration, ρ_{ice} and ρ_{water} are the densities of ice and water, respectively. ρ_{ice} is assumed constant in this calculation. Z_s and Z_{lake} are the elevations of the ice surface and the ice-water contact above sea-level. The ice surface elevation and lake elevation can be calculated from airborne laser altimeter and ice-penetrating radar data. Figure 1 shows the grid of flight lines above Lake Vostok where ice surface elevation and ice thickness data are available (Studinger et al., 2003).

Kapitsa et al.'s (1996) original salinity estimate was limited by the ice thickness and ice surface elevation data sets available at the time. During the 2000/01 austral summer more than 21,000 line km of airborne ice-penetrating radar and laser altimeter measurements have been collected (Studinger et al., 2003) providing a much more robust basis for estimating the salinity of subglacial Lake Vostok. Figure 1 shows the calculation of the hydrological potential Φ across Lake Vostok where a lake reflector has been identified on radar data, i.e. the ice is floating. Using a mean ice density ρ_{ice} = 913 kg/m^3 (Kapitsa et al., 1996), and a water density ρ_{water} that takes into account the compressibility of water (at S = 0 ‰) depending on the ice overburden pressure p_{ice} , the calculation differs only from Kapitsa et al.'s (1996) work by using the grid of airborne ice-penetrating radar and laser altimeter data above Lake Vostok (Figure 1) instead of the SPRI radar flight and ERS-1 altimeter measurements. Figure 1 shows that the hydrological potential Φ calculated following Kapitsa et al.'s approach (1996) is not constant but rather reveals systematic changes across the lake. The hydrological potential increases from the south to the north and also generally increases towards the grounding line (Figure 1). The northern part of the lake shows a 10-km-wide zone around the grounding line with elevated hydrological potential. As mentioned by Kapitsa et al. (1996) the hydrological potential in regions near the groundling lines could be affected by boundary stresses and might need to be excluded from the calculations when estimating the salinity. However, the data along flight 130 that Kapitsa et al. (1996) used to calculate the salinity is close to the upglacier grounding line and only reaches the undisturbed center of the lake over a short segment in the northern part (see Figure 1 in Kapitsa et al. (1996)). Thus, their calculation of the salinity might have been affected by edge effects.

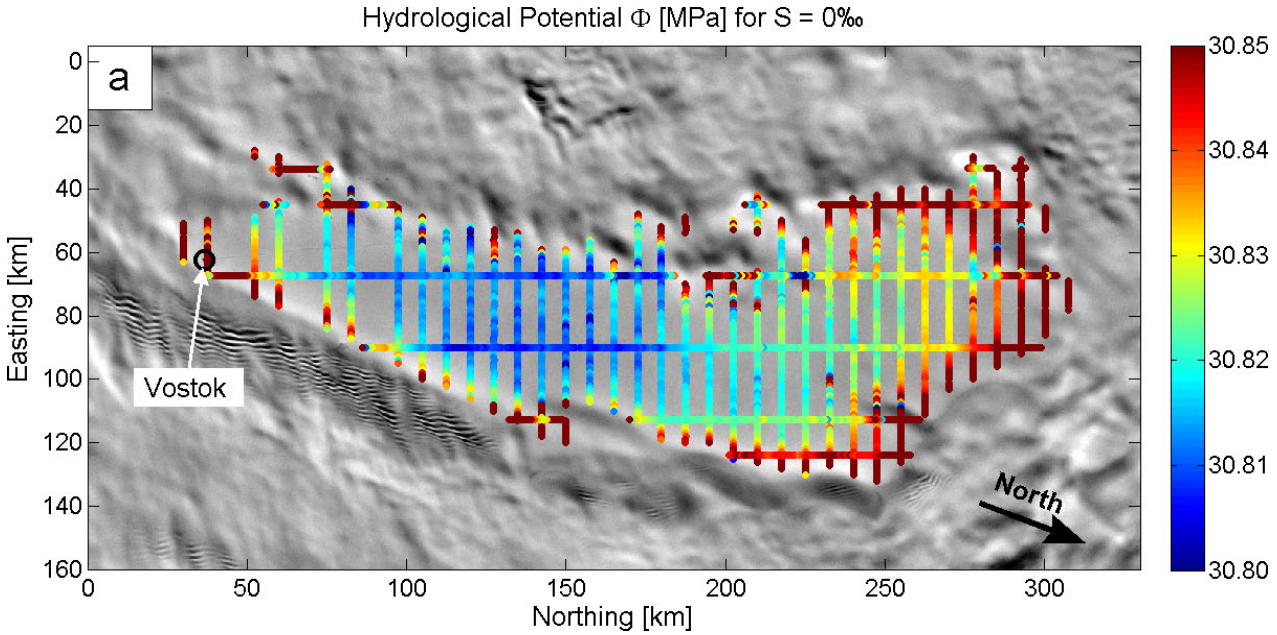

Figure 1. Hydrological potential Φ in MPa of subglacial Lake Vostok calculated using Equation 1. The ice density ρ_{ice} = 913 kg/m^3 is the mean density used by (Kapitsa et al., 1996). The water density assumes a salinity S = 0 ‰ and includes compressibility. Aerogeophysical data are described in Studinger et al. (2003). Basemap image is MODIS mosaic distributed by NSIDC.

The systematic change in hydrological potential across the lake, calculated using a first order approach, suggests that some of the parameters are not constant as assumed but vary across the lake. In order to understand the magnitude of this deviation, it is useful to reverse the calculation and predict the ice surface elevation from Equation 1 using a constant hydrological potential across the lake. The difference between the observed ice surface elevation, measured from airborne laser altimeter data $Z_{s(laser)}$, and the predicted ice surface elevation $Z_{s(model)}$, calculated from Equation 1 assuming Φ = const. and S = 0 ‰, ranges from -3 to +3 m. The difference between the predicted and measured ice surface elevation is a measure for the deviation from the assumption underlying Equation 1. The observed differences are smaller than the estimated uncertainty in ice thickness estimates of ± 16 m (Bell et al., 2002) and could simply be caused by noise in the data. However, the coherent spatial pattern of changes in Figure 1 suggests that the variation is real rather than artificial.

The observed pattern of deviations is remarkably similar to the bathymetric structure of subglacial Lake Vostok. Studinger et al. (2004) used aerogravity data to estimate the depth and shape of the water cavity. Figure 2 shows that Lake Vostok consists of two sub-basins separated by a ridge with very shallow water depths. The deeper southern sub-basin is approximately double the spatial area of the smaller northern sub-basin. The distribution of melting and freezing at the base of the ice sheet appears to be intimately linked to the two basin structure (Figure 2). The regions with basal melting and freezing have been estimated from thickness changes between internal layers along ice flow (Bell et al., 2002; Tikku et al., 2004). Over the northern basin, basal melting is dominant while over the southern basin, basal freezing characterizes the lake/ice interaction. The intimate link between the regions of melting and freezing and the bathymetric structure of the lake has important ramifications for the water circulation. Studinger et al. (2004) hypothesized that the lake chemistry, biology, and salinity between the two basins could be different because of limited water exchange between the two basins.

The pattern of melting and freezing and the bathymetric structure of the lake are very similar to variations in hydrological potential shown in Figure 1 which may indicate a link between water circulation, melting and freezing and salinity. It is intriguing to speculate whether the observed variations in Figure 1 between the northern and southern part of the lake are caused by differences in salinity of the lake. In order to answer this question several effects have to be included in a refined calculation of the hydrological potential:

- A firn layer has to be included in the calculation of ice thickness from radar wave travel times. Because the velocity v of electromagnetic waves in firn is faster than in ice ($v_{firn} > v_{ice}$) a firn correction has to be added to the preliminary ice thickness estimates. Including a firn layer will impact the ice overburden pressure estimate by changing the total ice thickness estimate and reducing the load by a near surface layer with lower density.

- Lateral changes in the radar wave velocity for the deeper section of the ice sheet have to be accounted for.
- The vertical density structure of the ice $\rho_{ice} = \rho_{ice}(z)$ has to be included in the calculation of the ice overburden pressure p_{ice} . The water density is a function of the salinity, temperature, and pressure, i.e. $\rho_{water} = \rho_{water}(S, T, p_{ice})$.

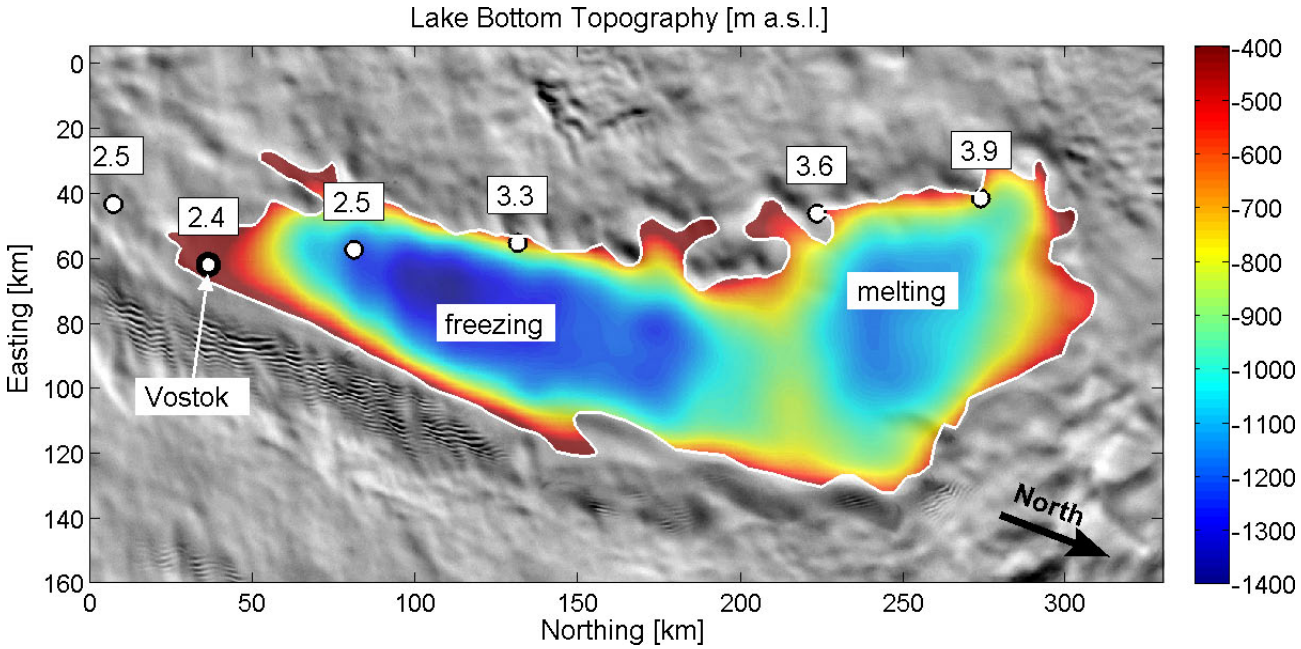

Figure 2. Lake bottom topography in m a.s.l. estimated from aerogravity data (Studinger et al., 2004). Lake Vostok is separated into two sub-basins, a larger and deeper basin in the south and a northern, smaller and shallower basin. The bathymetric structure coincides with the pattern of melting and freezing at the base of the ice sheet (Tikku et al., 2004). Meltwater will be introduced predominately into the northern basin and lake water will be removed by freezing from the southern basin. The pattern of melting and freezing and the bathymetric structure are similar to the variations in hydrological potential shown in Figure 1 and may indicate a link between water circulation, melting and freezing and salinity. Numbers are annual snow accumulation rates in cm/yr ice equivalent from Dahe et al. (1994). Basemap image is MODIS mosaic distributed by NSIDC.

Firn correction

Because the velocity v of electromagnetic waves in firn is faster than in ice ($v_{firn} > v_{ice}$), the ice thickness estimate (h_{ice}) using the two-way traveltime (t) of the radar waves assuming a constant velocity for electromagnetic waves in ice is:

$$h_{ice} = \frac{\left(t_{bed} - t_{surface}\right) v_{ice}}{2} + \Delta z_{firn} \qquad (2)$$

with Δz_{firn} being the firn correction added to the preliminary depth calculation based on the assumption of constant velocity in solid ice. For this purpose the thickness of the firn layer (h_{firn}) is often assumed as the pore close-off depth (PCOD). At Vostok, the open pores diminish between 90 and 102 m depth (Bender et al., 1994) resulting in h_{firn} (Vostok) = 102 m. The air spaces between grains usually close of at a density ρ_{ice} (h_{firn}) = $\rho_{PCOD} \approx 830$ kg/m^3. The remaining air (about 10% by volume) is now present as air bubbles and the firn has become glacier ice (e.g., Paterson, 1994). A further slow increase in density with depth results from compression of the air bubbles by creep of the surrounding ice. The density variation with depth $\rho_{ice}(z)$ is known from the Vostok ice core for the near surface part (Lipenkov et al., 1997); Figure 3). In order to calculate Δz_{firn}) and for a later discussion of lateral changes in the thickness of the firn layer it is convenient to fit an empirical function through the observed density values. A density-depth relationship has been derived by Herron and Langway (1980), based on an empirical model of the densification of firn.

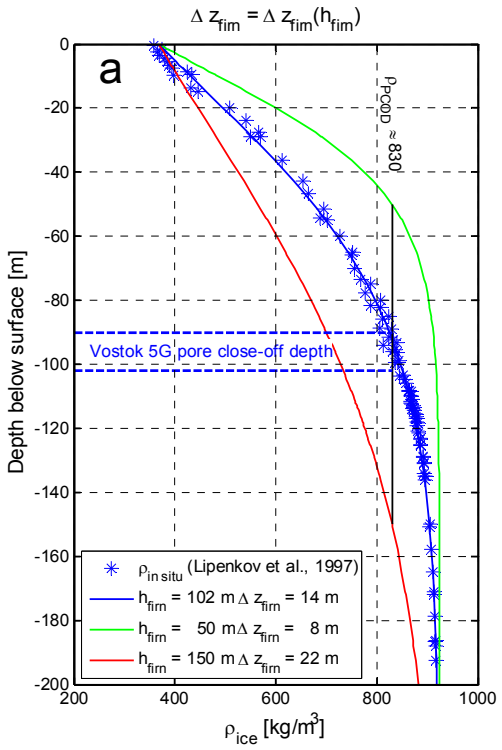

Figure 3. Firn correction Δz_{firn} calculated for 3 different density-depth relations corresponding to h_{firn} = 50 m (green curve, hypothetical), h_{firn} = 102 m (blue curve, Vostok 5G), and h_{firn} = 150 m (red curve, hypothetical). The pore-closure density $\rho_{PCOD} = \rho_{ice}(h_{firn}) \approx 830$ kg/m^3 for h_{firn} = 50 m and h_{firn} = 150 m was estimated from the least-squares fit of the Vostok density data (r^2 = 99.66%) and coincides with commonly cited values in the literature (e.g., Paterson, 1994). *In situ* density data are from Lipenkov et al. (1997). Vostok 5G pore close-off depth (thickness of firn layer) is from Bender et al. (1994) (blue dashed lines).

The model is only valid for the upper parts of an ice sheet, since it does not account for the thinning of annual layers by plastic flow (Nye, 1963).

Results: Estimating the salinity of subglacial lakes

Because of the importance of the salinity for numerical circulation models, the interpretation of accreted ice samples, and future plans to sample the waters of subglacial Lake Vostok the goal of this project is to estimate the salinity of 3 large subglacial lakes in Antarctica from aerogeophysical data. The density of water ρ_{water} can be estimated from Equation (1) or alternatively from the slope of the ice surface elevation plotted against the ice thickness (Kapitsa et al., 1996). The density of water depends on the salinity S, the temperature T and the pressure (here ice overburden pressure p_{ice}): $\rho_{water} = \rho_{water}(S, T, p_{ice})$. If the temperature and pressure are known, the salinity can be inferred from the water density using the equation of state for water (UNESCO, 1981). The temperature of the water is unknown, however, the temperature at the ice/water interface can be estimated by assuming that it is at the melting temperature $T_{pmp} = -c_T p_{ice}$ with c_T being the pressure melting coefficient. Alternatively, a water temperature of -3.1°C predicted by linear extrapolation of the Vostok temperature gradient will be used (Souchez et al., 2000).

As shown above the input parameters for Equation (1) are not independent and the challenge in estimating the salinity will be to separate the impact of the uncertainty in each measurement on the salinity estimate. The sensitivity of each measurement will be evaluated by estimating the salinity for a prescribed range of the parameter and keeping all other parameters constant. This will be done for every parameter involved in the calculation of the salinity. It may not be possible to distinguish, for example, if a change in hydrological potential observed in Figure 1 is caused by changes in thickness of the firn layer or changes in the radar velocity in the deeper sections of the ice sheet, but it will be possible to estimate a range of salinities by varying these parameters within reasonable boundaries.

Acknowledgements. Vladimir Ya. Lipenkov (Arctic and Antarctic Research Institute, St. Petersburg, Russia) is thanked for providing the Vostok ice core density data and for discussions. Funding for this work was provided by the U.S. National Science Foundation award ANT-06-36584.

References

Bell, R. E., et al. (2002), Origin and fate of Lake Vostok water frozen to the base of the East Antarctic ice sheet, *Nature*, *416*, 307-310.

Bender, M. L., et al. (1994), Changes in the O_2/N_2 ratio of the atmosphere during recent decades reflected in the composition of air in the firn at Vostok Station, Antarctica, *Geophys. Res. Lett.*, *21*, 189-192.

Dahe, Q., et al. (1994), Distribution of Stable Isotopes in Surface Snow Along the Route of the 1990 International Trans-Antarctica Expedition, *J. Glaciol.*, *40*, 107-118.

Herron, M. M., and C. C. Langway (1980), Firn densification: an empirical model, *J. Glaciol.*, *25*, 373-385.

Kapitsa, A. P., et al. (1996), A large deep freshwater lake beneath the ice of central East Antarctica, *Nature*, *381*, 684-686.

Lipenkov, V. Y., et al. (1997), Bubbly-ice densification in ice sheets; II, Applications, *J. Glaciol.*, *43*, 397-407.

Nye, J. F. (1963), Correction factor for accumulation measured by the thickness of the annual layers in an ice sheet, *J. Glaciol.*, *4*, 785-788.

Paterson, W. S. B. (1994), *The physics of glaciers. 3 ed*, 480 pp., Elsevier Science, Oxford, United Kingdom.

Souchez, R., et al. (2000), Ice formation in subglacial Lake Vostok, central Antarctica, *Earth Planet. Sci. Lett.*, *181*, 529-538.

Studinger, M., et al. (2003), Ice cover, landscape setting, and geological framework of Lake Vostok, East Antarctica, *Earth Planet. Sci. Lett.*, *205*, 195-210.

Studinger, M., et al. (2004), Estimating the depth and shape of subglacial Lake Vostok's water cavity from aerogravity data, *Geophys. Res. Lett.*, *31*, L12401.

Tikku, A. A., et al. (2004), Ice flow field over Lake Vostok, East Antarctica inferred by structure tracking, *Earth Planet. Sci. Lett.*, *227*, 249-261.

UNESCO (1981), Tenth report of the joint panel on oceanographic tables and standards, *UNESCO Technical Papers in Marine Science*, *36*, 13-21.